Determining Limonene Diffusion in Molten Polyethylene from within 0.1 μs Molecular Dynamics Trajectories

G. E. Karlsson, T. S. Johansson, U. W. Gedde, and M. S. Hedenqvist*

Royal Institute of Technology, Department of Polymer Technology, SE−100 44 Stockholm, Sweden

Received January 14, 2002; Revised Manuscript Received May 31, 2002

ABSTRACT: Molecular dynamics simulations of the diffusion of limonene into molten polyethylene were performed in order to explore the possibility of using atomistic simulations to predict the diffusion of "larger" solute molecules in polymers. The system contained 6000 anisotropic united atom methylene units with a molar mass of 84 000 g mol^{-1}. A "united atom" limonene molecule (C_{10} H_{16}) was introduced into the polyethylene matrix. Limonene trajectories were generated for 2−100 ns at 77−227 °C. The simulated diffusivities were compared with experimental zero-concentration diffusivities of limonene in natural rubber and ultrahigh molar mass polyethylene, obtained from desorption measurements in the same temperature range. The simulated diffusivities and activation energy were within 30% and 16% of the experimental thermodynamic diffusivities and activation energies, respectively. The simulated average diffusivities, obtained from 10 trajectories, changed by only 33% when the simulation time was shortened from 100 ns to 500 ps. The limonene molecule "vibrated" in a cagelike fashion on a 1−2 ps scale, whereas on a larger time scale the jumping was liquidlike. The limonene molecule showed tumbling during its motion through the polyethylene matrix.

Introduction

There are currently specific limitations of approximately 200 substances which are permitted by the EC directives as additives for use in plastics in contact with food.[1] The list is increasing continuously and is expected to include several thousands of chemicals in the near future. The cost for the development of experimental methods to determine the migration rates in order to meet the limitations will be very high. There is thus a need for alternative methods to obtain chemical migration data, e.g., computer-based simulations.

Molecular dynamics (MD) simulation has proven useful for predicting properties of polymers, e.g., *PVT* data, dielectric permittivity, solubility parameters, the solubility of small-molecules, X-ray diffraction patterns, and molecular characteristic ratios.[2] MD has also been used to obtain the diffusivities of small gas molecules in polymers.[3] Of particular interest here is the potential to predict diffusivities of larger molecules using MD simulation.[4] The prediction of the migration rates of larger molecules, e.g., antioxidants and aroma compounds, requires that the simulated molecular system is large and possibly also that the system has to be followed for a long time. To avoid unwanted correlations between the periodic boundaries and the trajectory of the guest molecule, the side of the box containing the polymer should be at least twice as large as the size of the guest molecule.

In the present study, limonene has been chosen as the migrating molecule and the polymer matrix is a 6000 anisotropic-united-atom (AUA) polyethylene (PE) system. The migration properties of limonene are of practical interest, because it is the major aroma constituent in citrus fruit juices and it readily migrates from the liquid into polyethylene-based packaging materials causing a deterioration in the quality of fruit juice.[5] A more general purpose of this study was to test the prediction capability of MD simulation in determining the diffusivity of larger solute molecules.

Experiments and Simulations

Desorption Measurements. (*R*)-(+)-Limonene (D-limonene) was purchased from Aldrich (purity >97%). The samples studied were an ultrahigh molar mass PE ($\bar{M}_w$ > 1040 000 g mol^{-1}, $\bar{M}_w/\bar{M}_n$ = 54.45, mass crystallinity w_c = 0.59) and a sulfur-cross-linked natural rubber (NR, molar mass of uncross-linked polymer, $\bar{M}_w$ = 664 000 g mol^{-1}, $\bar{M}_w/\bar{M}_n$ = 4.6. $\bar{M}_c$ = 2500 g mol^{-1} at 25 °C as determined from *n*-hexane sorption equilibrium data). PE was melt-crystallized during cooling at a rate of 15 °C min^{-1} from 200 °C in a Schwabenthan compression molding machine (Polystat 400s).

The dimensions of the unswollen samples used in the desorption experiments were as follows: PE, thickness = 1.0 mm, width = 40 mm, length = 40 mm; NR, 2.715−3.46 mm × 40 mm × 40 mm. The samples were saturated in liquid limonene (ρ_l = 840 kg m^{-3} (25 °C)) at 20−177 °C. After sorption equilibrium was established, the surface-dried samples were exposed to air at 20−227 °C, and the desorption was monitored by intermittent weighing of the samples on a Mettler AE balance after different times. Since the specimens had been exposed to liquid limonene during the sorption operation, the solubility and diffusivity of limonene were measured in materials "cleaned" with respect to low-molar mass oligomers and additives. The amount of material extracted during the immersion in the liquid was less than 12% in the case of NR and less than 1% in the case of PE.

The desorption curves were fitted to Fick's second law of diffusion for a plate geometry:[6]

$$\frac{\partial C}{\partial t} = \frac{\partial}{\partial x}\left(D(C)\frac{\partial C}{\partial x}\right) \tag{1}$$

where C is the penetrant concentration (g cm^{-3}), x is the thickness coordinate (cm), and t is time (s). Only half the plate thickness ($2L$) was considered. The inner boundary coordinate was described as an isolated point

$$\left(\frac{\partial C}{\partial x}\right)_{x=L} = 0 \tag{2}$$

and the outer boundary was allowed to take any type of

* To whom correspondence should be addressed.

10.1021/ma0200569 CCC: $22.00
Published on Web 08/10/2002

Table 1. Potential Energy Parameters for PE[a]

function	parameters	
bond stretch energy = $^1/_2 k_R(r - r_0)^2$		
C−C	$k_R = 663$	$r_0 = 1.54$
bond bending energy = $^1/_2\ k_\theta(\theta - \theta_0)^2$		
C−C−C	$k_\theta = 482$	$\theta_0 = 111.6°$
torsional potential = $^1/_2 V_3[1 + \cos(3\phi)] + ^1/_2 V_1[1 + \cos(\phi)]$		
C−C−C−C	$V_3 = 13.4$	$V_1 = 3.35$
nonbonded potential = $4\sum_{i<j}\epsilon_{LJ,ij}[(\sigma_{ij}/r_{ij})^{12} - (\sigma_{ij}/r_{ij})^6]$		
−C−	$\epsilon_{LJ} = 0.686$	$\sigma = 3.51$

[a] Energies in kJ mol^{-1}, distances in angstroms, and angles in radians (equilibrium values shown above as degrees). Parameter values from Pant et al.[9] The k_R values given are reduced by a factor of 4 compared to spectroscopic values to increase the computation speed.

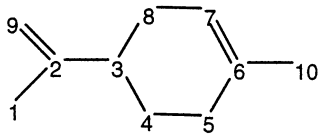

Figure 1. Limonene molecule and the carbon numbers.

function. During desorption, evaporation takes place at the surface

$$D(C)\left[\frac{\partial C}{\partial x}\right]_{x=0} = F_0 C \tag{3}$$

where F_0 is the evaporation constant determined to be between 5×10^{-6} and 5×10^{-5} cm s^{-1} for both materials using a procedure of Bakhouya et al.[7] The concentration-dependent diffusivity was described as

$$D(C) = D_{co}e^{\alpha C} \tag{4}$$

where D_{co} is the zero concentration diffusivity and α is the plasticization power.[6] Equations 1−4 were solved by a stable implicit finite-difference method described in ref 8.

Molecular Dynamics Simulations. The PE system used in the simulation consisted of a single chain with 6000 anisotropic united atom (AUA) methylene units, corresponding to a molar mass of 84 000 g mol^{-1}. The limonene molecule (Figure 1) was defined as consisting only of united-atoms of repeating methyl, methylene and carbon units. The simulations were performed using an own Fortran computer code, originating from Boyd,[9] and also the GROMACS 3 software.[10,11] The *PVT* behavior was generated using constant particle, pressure, and temperature (*NPT*) dynamics, and the diffusion trajectories were collected using constant particle, volume, and temperature (*NVT*) dynamics. The weak coupling scheme[12,13] was used with the temperature coupling constant (τ_T) set to 5 fs and a pressure coupling (τ_P/β) set to 1×10^4 for *NPT*. The time integration was performed using either the velocity-verlet or the leapfrog algorithm.[13] The actual choice of integration method was of no importance here. A time step of 1 fs was used at all temperatures.

The packed polyethylene system was made from an all-trans chain placed in a large periodic cubic box (box side = 700 Å). The box was shrunk to equilibrium size at a high temperature (377 °C) and a pressure of 0 bar. The box was shrunk in steps using *NPT* dynamics. After each step, the system was allowed to equilibrate under *NVT* dynamics for 50 ps in order to ensure cooling under "relaxed" conditions and also to ensure space filling of the box. Lower temperatures were obtained by cooling. The limonene molecule was inserted in the polyethylene box before the polyethylene system had condensed to its final size, when the box contained sufficient free volume. Subsequently the box was shrunk to equilibrium size by the same procedure as was used for the pure PE system. Volume equilibration was obtained by generating trajectories for at least 2 ns at each temperature.

The computations were carried out on 800 MHz Pentium III 2-processor PC's.

The potential function parameters used for PE and limonene are listed in Tables 1 and 2. The potential function parameters for PE were obtained from Pant et al.,[9] and the potential function parameters for limonene were based on the DREIDING force field.[14] Bond stretches, bond-bending vibrations, out-of-plane vibrations (oop), torsional motions, nonbonded Lennard-Jones types of forces, and atomic velocities contributed to the total energy (U_{tot}) and forces in the system

$$U_{tot} = U_{bond} + U_{bend} + U_{oop} + U_{tors} + U_{non-bond} + U_{kin} \tag{5}$$

which may be written explicitly as

$$U_{tol} = \sum_{i,j}\frac{1}{2}k_{R_{ij}}(r_{ij} - r_{0ij})^2 + \sum_{i,j,k}\frac{1}{2}k_{\theta_{ijk}}(\theta_{ijk} - \theta_{0_{ijk}})^2 + \sum\frac{1}{2}k_0\delta^2 + \sum_{i,j,k,l}\frac{1}{2}(V_{a1}[1 + V_{a2}\cos(V_{a3}\phi_{ijkl})] + V_{b1}[1 + V_{b2}\cos(V_{b3}\phi_{ijkl})]) + \sum_{i<j}4\epsilon_{LJ_{ij}}\left[\left(\frac{\sigma_{ij}}{r_{ij}}\right)^{12} - \left(\frac{\sigma_{ij}}{r_{ij}}\right)^6\right] + \sum_i\frac{1}{2}m_i\left(\frac{\partial r_i}{\partial t}\right)^2 \tag{6}$$

The truncation radii for the nonbonded forces and neighbor-list search were set to 9.0 Å. Continuum corrections for the truncation of energy and pressure were applied.

Results and Discussions

For a reliable prediction of the limonene diffusivity, it is important that the simulated system has a proper density. Figure 2 shows that the simulated specific volumes were within 1−2.5% of the experimental values reported for linear polyethylenes.[15,16] The simulated thermal expansion coefficient in the melt region was in close agreement with experiment. Figure 3 shows that the equilibration times were short, even though the simulated system was large. To explore whether there was a risk that the simulated molecular system was frozen-in by too rapid equilibration, the system at 77 °C was rapidly and "slowly" (1 °C ps^{-1}) cooled from 127 to 77 °C, and the specific volumes of these systems were compared. Figure 3 shows that both systems had the same specific volumes, which indicated that the rapidly cooled system was not frozen-in. The effects on the final specific volume of using different initial atom velocities was investigated and it was shown that the magnitude and distribution of initial atom velocities had no influence on the *PVT* properties of the "equilibrated" systems.

The diffusivity of limonene was obtained by monitoring the mean square displacement of the center-of-mass

Table 2. Potential Energy Parameters for Limonene[a]

function	parameters		
bond stretch energy = $^1/_2 k_R(r - r_0)^2$			
1−2, 2−3, 5−6, 7−8, 6−10	$k_R = 2929$	$r_0 = 1.43$	
3−4, 4−5, 3−8	$k_R = 2929$	$r_0 = 1.53$	
6−7, 2−9	$k_R = 5858$	$r_0 = 1.33$	
bond bending energy = $^1/_2 k_\theta(\theta - \theta_0)^2$			
1−2−3, 1−2−9, 3−2−9, 5−6−7, 5−6−10, 6−7−8, 7−6−10	$k_\theta = 418.4$	$\theta_0 = 120°$	
2−3−4, 2−3−8, 3−4−5, 3−8−7, 4−5−6, 4−3−8	$k_\theta = 418.4$	$\theta_0 = 109.5°$	
torsional energy = $^1/_2 V_n[1 + \cos(n\phi - \phi_0)]$			
1−2−3−4, 1−2−3−8, 4−3−2−9, 8−3−2−9	$n = 6$	$V_n = 0.523$	$\phi_0 = 180°$
2−3−4−5, 2−3−8−7, 4−3−8−7, 5−4−3−8	$n = 3$	$V_n = 2.092$	$\phi_0 = 0°$
3−4−5−6	$n = 3$	$V_n = 4.184$	$\phi_0 = 0°$
3−8−7−6	$n = 6$	$V_n = 2.092$	$\phi_0 = 180°$
4−5−6−7, 4−5−6−10	$n = 6$	$V_n = 1.046$	$\phi_0 = 180°$
5−6−7−8, 8−7−6−10	$n = 2$	$V_n = 47.07$	$\phi_0 = 180°$
out of plane energy = $^1/_2 k_0\delta^2$			
2−1−3−9, 6−5−7−10	$k_0 = 167.4$	$\delta = 0°$	
3−4−2−8	334.7	$\delta = 35.3°$	
nonbonded potential = $4\sum_{i<j}\epsilon_{LJ,ij}[(\sigma_{ij}/r_{ij})^{12} - (\sigma_{ij}/r_{ij})^6]$			
C	$\epsilon_{LJ} = 0.398$	$\sigma = 3.47$	
CH	$\epsilon_{LJ} = 0.614$	$\sigma = 3.55$	
CH_2	$\epsilon_{LJ} = 0.83$	$\sigma = 3.62$	
CH_3	$\epsilon_{LJ} = 1.046$	$\sigma = 3.70$	

[a] Energies in kJ mol^{-1}, distances in angstroms, angles in radians (equilibrium values shown above as degrees). Parameter values from Maya et al.[14]

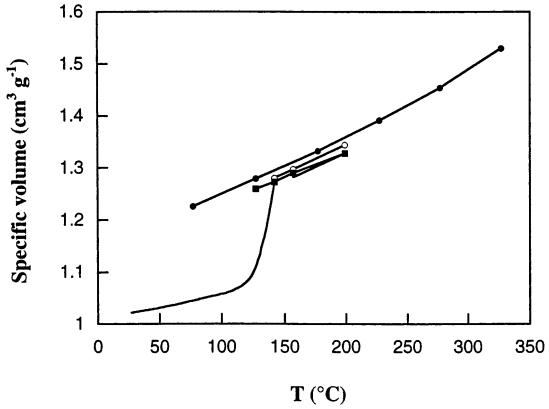

Figure 2. Specific volume as a function of temperature at 0 atm: (●) simulated data, (○) linear high-molar mass PE (■); branched PE; (−) linear medium-molar mass PE.

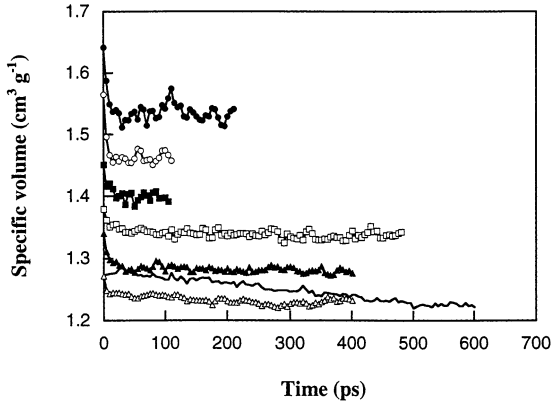

Figure 3. PE specific volume as a function of time at 327 (●), 277 (○), 227 (■), 177 (□), 127 (▲), and 77 °C (△, rapidly cooled; −, slowly cooled).

from the origin ($\bar{r}_0$) as a function of time:[17,18]

$$D_s = \frac{\lim_{t\to\infty}\langle(\bar{r}(t) - \bar{r}_0)^2\rangle}{6t} \qquad (7)$$

The averaging was done by generating new starting points every 10 ps along the trajectory. Figure 4 shows the mean square displacement as a function of time at 177 °C. The curve was approximately linear for times shorter than 60 ns. The curve shape was similar to that of the mean square displacement-time curves of melts of short PE chains.[19] The diffusion process was liquidlike rather than cagelike at these high temperatures. The limonene molecule thus tended to "flow" with the motion of the PE units. The jump maps of limonene presented in Figure 5 shows patterns typical of liquidlike flow, i.e., the discrete, in time well-separated jumps were absent. The jumps were based on differences in "mean" limonene positions calculated at 3 ps intervals. The limonene coordinates within the 3 ps intervals were collected every 10 fs. The 3 ps intervals were chosen because the lateral motion of limonene was decorrelated within 3 ps. The curve shape of the velocity auto correlation functions at 77 and 227 °C indicated that

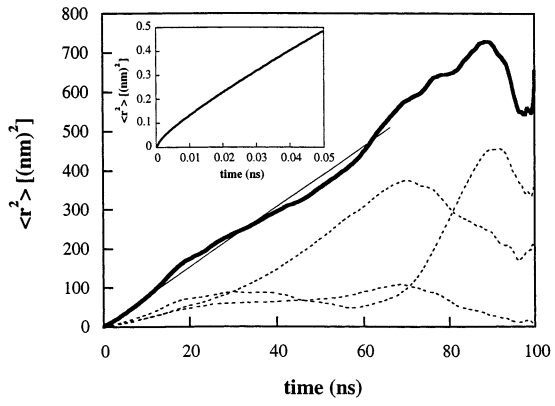

Figure 4. Mean square displacement from the origin as a function of time for limonene in polyethylene at 177 °C (solid thick line). The broken lines correspond to the average square displacement curve projected in the three orthogonal directions. The thin solid line shows the slope from where the diffusivity was calculated.

the limonene molecule changed its diffusive direction within 1−2 ps. The nonlinear initial slope shown in the insert graph of Figure 4 revealed a cagelike motion on these short time scales. The reorientations of the two

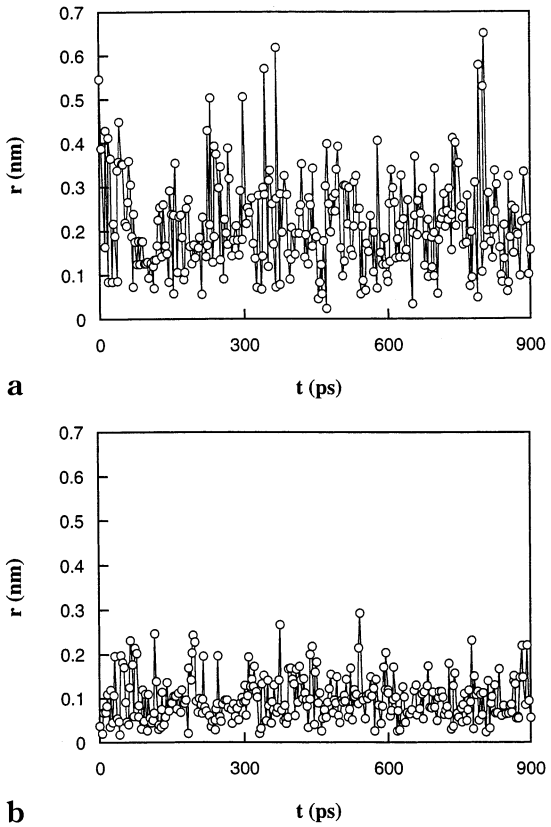

Figure 5. (a) Jump map for limonene at 227 °C. The displacement was calculated between successive 3 ps positional averages. (b) Jump map for limonene at 77 °C. The displacement was calculated between successive 3 ps positional averages.

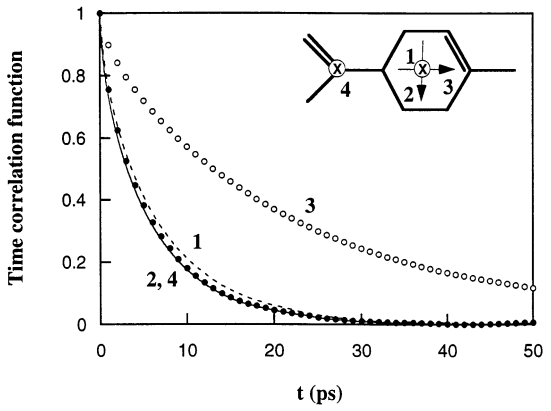

Figure 6. Time correlation functions for four different limonene vectors at 177 °C based on a 100 ns run.

orthogonal in-plane vectors and the two vectors normal to the planes defined by the carbons 4, 6, and 8 and 1, 2 and 9, respectively, were monitored through time-correlation functions (eq 8, Figure 6). The correlation times (τ) of the in-plane and ring-normal vectors yield information on the tendency for "spinning" and "tumbling" motions, respectively. The Kohlrausch−Williams−Watts (KWW) function was used to fit the time-correlation function[20]

$$\langle \mathbf{u}(t)\mathbf{u}(0)\rangle \approx e^{-(t/\alpha)^{\beta}} \tag{8}$$

where $\mathbf{u}(0)$ and $\mathbf{u}(t)$ are the vectors at times 0 and t respectively (Figure 6). It was observed that all the time-correlation functions were well fitted with the KWW-function with β ranging between 0.79 and 0.83. The correlation time was obtained through the integral:[20]

$$\tau = \int_0^{\infty} e^{-(t/\alpha)^{\beta}}\, \partial t \tag{9}$$

The correlation times were 5.6 ps (bond connecting the ring to the three carbons), 5.8 ps (in-plane vector perpendicular to the long axis), 6.4 ps (ring-normal), and 22.0 ps for the in-plane vector along the long axis. Thus, the limonene molecule tumbles, rather than spins, while moving through the polymer matrix. This behavior was different from the reported spinning of benzene in swollen polystyrene at 27 °C.[20] The absence of bulky side groups on the benzene ring and its tendency to orient parallel to the polystyrene ring units yielded in-plane and ring-normal vector time correlations of 5.28 ps and 1.23 ns, respectively, for a polystyrene system with 16 w% benzene. Thus, the spinning tendency was much stronger than the tumbling tendency. The tumbling tendency became stronger in systems with higher benzene contents.

This analysis showed that all translational and re-orientational features of the limonene motion were "relaxed" within 200 ps, involving cagelike behavior (1−2 ps), liquidlike motion (>2−3 ps) and tumbling and spinning motions (≤200 ps).

Figure 4 shows that the displacement of limonene, projected in the three orthogonal directions, was the same over the first 5−7 ns (isotropic motion). Figure 7 illustrates the 100 ns limonene trajectory. It shows that the molecule traveled through six periodic boxes in two directions (X and Y) and through four boxes in the third direction (Z). The trajectory yielded a diffusivity of: 1.26×10^{-7} cm^2 s^{-1}. A 100 ns run is time-consuming on the computer and it is desirable to obtain the same information from shorter runs. The 100 ns limonene trajectory at 177 °C was therefore analyzed in shorter time intervals (Figure 8). The upper and lower limits of the diffusion coefficient in Figure 8 corresponded to the maximum and minimum slopes from 10 consecutive runs at each time interval (2 runs at 50 ns). The slopes were estimated over the "linear" part of the curve that was closest to the origin: 5−10 ns (50 ns run), 0.2−0.8 ns (5 ns), 10−50 ps (0.5 ns) and 2.5−8 ps (50 ps). The diffusivities obtained showed only a moderate change with simulation time (50 ps to 50 ns). As a result of these findings, the limonene trajectories at the other temperatures were taken during 2 ns.

Figure 9 shows the limonene desorption curves in the natural rubber and molten PE. The experimental desorption curves at all temperatures for both NR and PE were well described by the use of the exponential concentration-dependent diffusivity (eq 4). The curvature at short times was due to the slow evaporation of limonene from the specimen surface. The same curvature was observed for limonene desorption in PE. The plasticization power, and consequently the diffusion concentration dependence, decreased with increasing temperature. For PE, it decreased from 44 to 0 cm^3/g in the temperature interval 20−177 °C, and for NR, it decreased from 6.8 to 0.6 cm^3/g in the temperature interval 25−227 °C. The apparent zero-concentration diffusivity, i.e., the diffusivity calculated directly from the desorption curves (eq 4), does not correspond to the

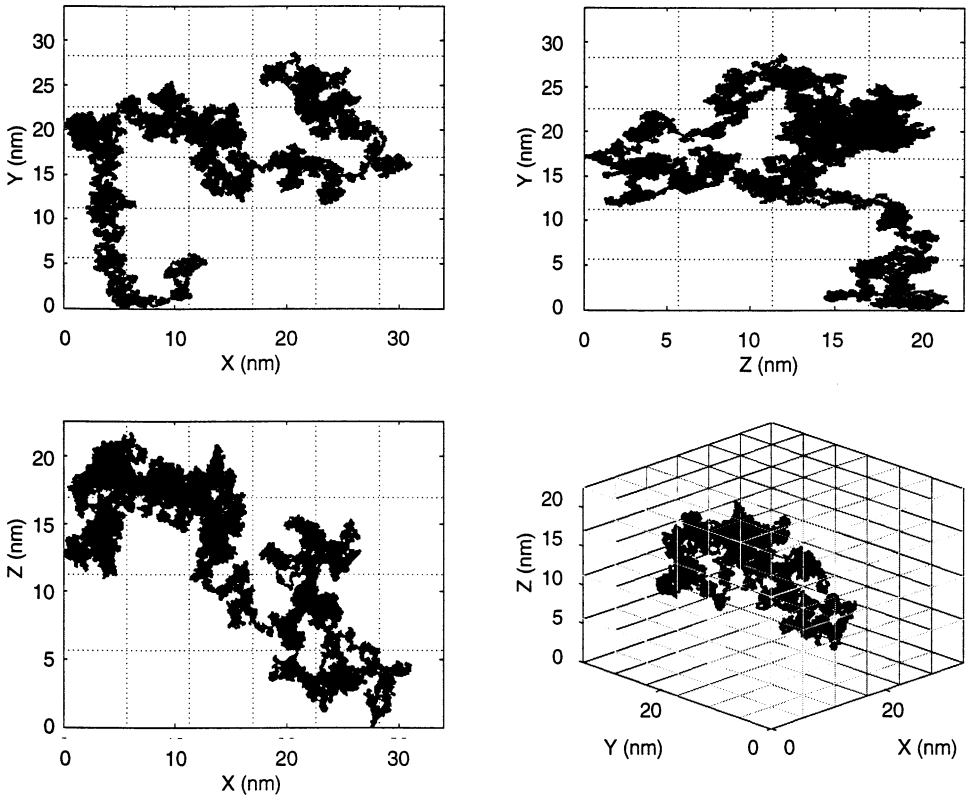

Figure 7. 100 ns limonene trajectory at 177 °C illustrated in two and three dimensions. The PE atoms are not displayed. The grid lines refer to the box size.

MD-simulated diffusivity. The apparent diffusivity is obtained in the presence of a limonene gradient and is not therefore equivalent to the limonene "self" diffusion coefficient obtained by MD simulation (eq 7). The self-diffusivity or thermodynamic diffusivity (D_T) is, however, related to the apparent (experimental) diffusivity (D) through a thermodynamic correction

$$D = D_T\left(\frac{\partial ln a_1}{\partial ln v_1}\right) \tag{10}$$

where a_1 is the solute activity. The correction is obtained by differentiating the Flory−Rehner equation[21]

$$\frac{\partial ln a_1}{\partial ln v_1} = (1 - v_1)(1 - 2\chi_{12}v_1) - \frac{\rho_2 V_1}{3\bar{M}_c(1 - v_1)^{\frac{2}{3}}} \tag{11}$$

where V_1, χ_{12}, and $\bar{M}_c$ are respectively the limonene molar volume, the Flory−Huggins interaction parameter and the number-average molar mass between crosslinks. For a semicrystalline polymer, the solute volume fraction (v_1) and the polymer density (ρ_2) refer to the amorphous component. All the necessary parameters in eq 11 were obtained from limonene solubility and NMR data of Marklund and Hedenqvist[22] (Table 3). $\bar{M}_c$ was determined from NMR data on a nitrile rubber NBR, 27% nitrile).[22] For PE, due to the difficulty of obtaining $\bar{M}_c$, the last term in eq 11 was omitted ($\bar{M}_c \rightarrow \infty$) and the effect of "crosslinks" was considered within the χ_{12} parameter. χ_{12} was obtained from the limonene solubility in the amorphous component in PE. The PE data at 20, 50 and 80 °C were taken from a high-density polyethylene (ρ = 0.941 at 20 °C). Because of the complexity of determining the crystallinity of the limonene-saturated PE at 80 °C, the χ_{12} value was estimated by interpolating χ_{12} between 25 and 177 °C. Parts a and b of Figure 10 show the simulated and experimental limonene diffusivity. To assess the prediction power of MD in this study, experimental and simulated diffusivities of other similar systems were also shown in the figures. Interestingly, the simulated limonene diffusivities were close to the limonene self-diffusion values in both natural rubber and molten polyethylene must, however, be pointed out that the degree of thermodynamic correction presented in Figure 10, parts a and b, is very uncertain due to the uncertainty of the input parameters in the Flory−Rehner equation (eq 9 and Table 3). Evidently MD is a promis-

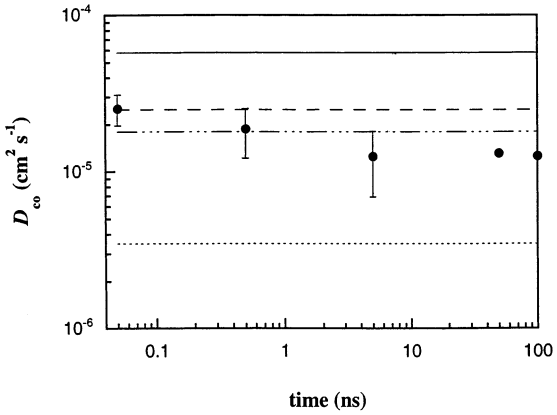

Figure 8. Calculated limonene diffusivity at 177 °C as a function of the simulation time. The solid line corresponds to simulated methane diffusivity in the same PE system. The dashed and dotted lines correspond to the simulated limonene diffusivities at 227 and 127 °C, respectively. The semi-dashed/semi-dotted line corresponds to experimental *o*-xylene diffusivity in molten PE at 175 °C.[23]

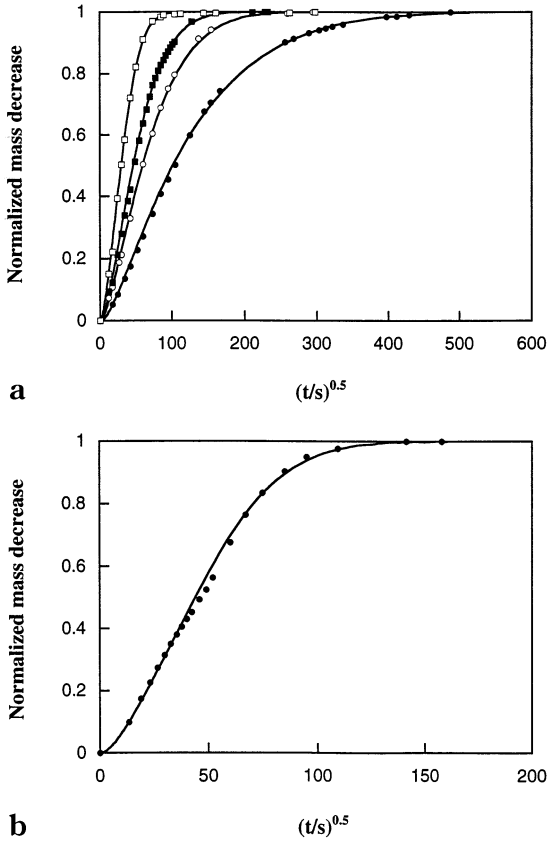

Figure 9. (a) Limonene desorption in NR as a function of time. The solid lines correspond to the fit of eq 4 to experimental data at 77 (●), 127 (○), 177 (■), and 227 °C (□). (b) Limonene desorption in PE at 177 °C as a function of time (●). The solid line corresponds to the fit of eq 4 to experimental data.

Table 3. Parameters in the Flory−Rehner Equation (Equation 9).[22]

material	T (°C)	ρ_2[a] (g cm^{-3})	V_1[b] (cm^3 mol^{-1})	$v_{1\infty}$[c]	χ_{12}[d]	$\bar{M}_c$[e] (g mol^{-1})
NR	77	0.970	167.4	0.413	0.84	5800
NR	127	0.934	173.4	0.469	0.77	7500
NR	177	0.900	179.5	0.524	0.70	8600
NR	227	0.864	185.9	0.579	0.53	9400
PE	20	0.941	160.8	0.109	1.07*	
PE	50	0.927	164.3	0.136	0.97*	
PE	80	0.907	167.7	0.447	0.87*	
PE	177	0.758	179.5	0.894	0.51*	

[a] Polymer density. [b] Limonene molar volume. [c] Saturation limonene volume fraction or maximum limonene volume fraction of desorption run. [d] Interaction parameter in eq 9. An asterisk indicates that the Flory−Huggins equation has been used ($\bar{M}_c \rightarrow \infty$) and that the effects of cross-links (crystals) are included in the interaction parameter. [e] Molar mass between cross-links. [e] Molar mass between cross-links on NBR. All PE data at 20 −80 °C are on a HDPE.

ing technique for predicting diffusivities of larger solutes, especially in view of that only relatively short runs seems necessary, at least for rough estimates (Figure 8). It is known that the use of the united atom concept may lead to higher diffusivities than that when explicit atoms are used. This seems to be of minor importance here, since the simulations yielded slightly lower diffusivities than the experiments.[17] The simulated activation energy for diffusion was 26 kJ mol^{-1} and the experimental activation energies in natural rubber and polyethylene were both 31 kJ mol^{-1} in the melt. The *o*-xylene zero-concentration diffusivities in molten polyethylene are also given and these values were close to the simulated and experimental limonene values.[23] The *o*-xylene activation energy was slightly lower (21 kJ mol^{-1}) than that of limonene, which seemed reasonable based on the fact that *o*-xylene (121 cm^3 mol^{-1}) is slightly smaller than limonene (162 cm^3 mol^{-1}).

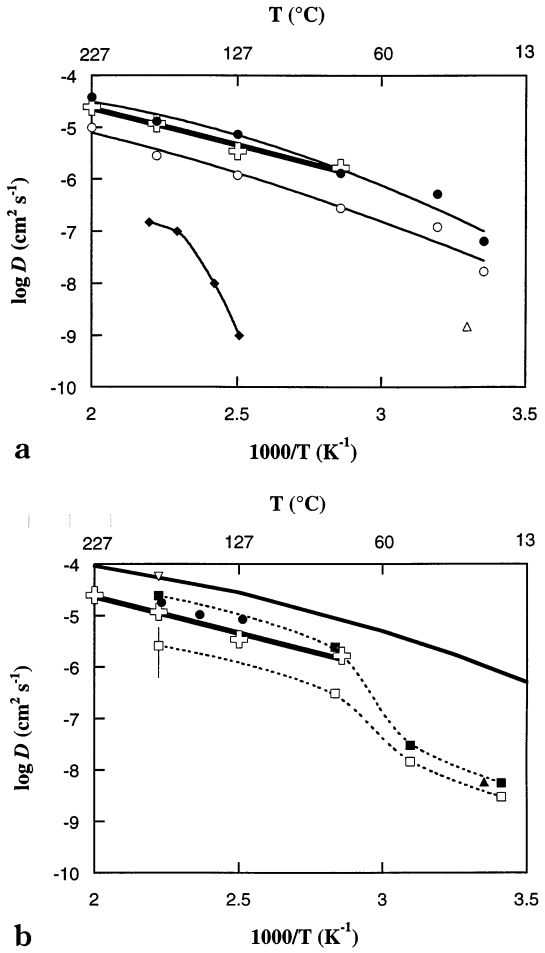

Figure 10. Simulated limonene (✣) diffusivity using eq 7 as a function of time together with the experimentally determined apparent limonene zero-concentration diffusivity (○) and the thermodynamic limonene zero-concentration diffusivity (●) in NR. The experimental values are averages of calculations based on dry and swollen thicknesses. ◆ refers to *o*-xylene zero-concentration diffusivities in polystyrene.[23] Also given is the limonene diffusivity (activity = 0.3) in oriented polypropylene[24] (△). (b) Simulated methane (▽) and limonene (✣) diffusivity using eq 7 as a function of time together with the experimentally determined apparent limonene zero-concentration diffusivity (□) and the thermodynamic limonene zero-concentration diffusivity (■) in PE. The experimental values are averages of calculations based on dry and swollen thicknesses. The solid line corresponds to simulated methane diffusivity in polyethylene from ref 2. ● refers to *o*-xylene zero-concentration diffusivities in molten PE [23] Also given is the apparent diffusivity of liquid limonene in LDPE[25] (▲). The vertical line corresponds to self-diffusion coefficients of C_{44} to C_{144} long paraffin chains, obtained by molecular dynamics simulations during 12 ns.[19]

Conclusions

The possibility of estimating diffusivities of larger solutes using atomistic simulations was tested. Here the force parameters for polyethylene were known, but the limonene molecule had to be constructed by force parameters from a general force field. From this point of view, the results were promising. The simulated

diffusivity and activation energy were within 30% and 16% of the experimental values, respectively. Note the uncertainty of thermodynamic correction. With today's PC power, a 100 ns run takes too long a time for practical reasons. Interestingly, however, a shortening of the simulation time by a factor of 200 yielded a drift in the average diffusivity, obtained from 10 trajectories, of only 33%. The diffusivity from a single trajectory, however, could be as much as 3−4 times that of the 100 ns run. The limonene molecule "vibrated" in a cagelike fashion on a 1−2 ps scale, whereas on a larger time scale the jumping was liquidlike. The limonene molecule moved through the PE matrix in a tumbling rather than spinning manner.

Acknowledgment. Elforsk, the Hans Werthén Foundation, and the Carl Tryggers Foundation are gratefully acknowledged for making this work possible. This study has also been sponsored by the Swedish Research Council of Engineering Sciences (TFR; Grant 97-125 doss 210) and the National Graduate School in Scientific Computing (NGSSC; Grant 200-97-24). Erik Lindahl, one of the persons behind the GROMACS 3 software, and Olle Edholm at the Department of Theoretical Biophysics, Royal Institute of Technology, are thanked for valuable discussions.

Nomenclature

$\mathbf{u}(0)$, $\mathbf{u}(t)$	vectors of the limonene molecule defined in Figure 8 at time 0 and t
$\bar{r}(t)$	limonene center-of-mass position at time t
$\bar{r}_0$	limonene center-of-mass original position
$\bar{M}_w$	mass average molar mass
$\bar{M}_c$	molar mass between cross-links
$\bar{M}_n$	number-average molar mass
α	the plasticization power
a_1	solute activity
C	solute concentration
$D(C)$	concentration-dependent diffusivity
D	apparent diffusivity
D_{co}	zero concentration diffusivity
D_s	MD-simulated diffusivity
D_T	thermodynamic or self-diffusivity
F_o	rate of evaporation
k_R, k_θ, k_0	elastic constants in the stretching, bending, and out-of-plane energy terms
L	thickness of half the plate
m	atom mass
r	bond length or interatomic distance
r_0	equilibrium bond length
T	temperature
t	time
U	energy
$v_{1,\infty}$	maximum or saturation solute volume fraction
V_1	solute molar volume
v_1	solute volume fraction
$V_{a,b}$	parameters in the torsional energy equation
x	space coordinate
α	constant describing the magnitude of concentration dependence of $D(C)$
β	stretched exponential constant
δ	out of plane angle
ϵ_{LJ}	Lennard-Jones force constant
ϕ	torsional angle
γ	stretched exponential constant
θ	covalent angle
θ_0	equilibrium covalent angle
σ	atom diameter or interatomic distance in the Lennard-Jones equation
τ	correlation time

References and Notes

(1) 90/128/EEC, E. D. *Official Journal of the European Committee* **13/12**−**90**, No. L 349/26.
(2) Boyd, R. H. *Trends Polym. Sci.* **1996**, *4*, 12.
(3) Han, J.; Boyd, R. H. *Polymer* **1996**, *37*, 1797.
(4) Hahn, O.; Mooney, D. A.; Müller-Plathe, F.; Kremer, K. *J. Chem. Phys.* **1999**, *111*, 6061.
(5) Paik, J. S. *J. Agric. Food Chem.* **1992**, *40*, 1822.
(6) Crank, J. *The Mathematics of Diffusion*; Clarendon Press: Oxford, England, 1986.
(7) Bakhouya, A.; Brouzi, A. E.; Bouzon, J.; Vergnaud, J. M. *Plast. Rubber Comput. Proc. Appl.* **1993**, *19*, 77.
(8) Hedenqvist, M. S.; Krook, M.; Gedde, U. W. *Polymer* **2002**, *43*, 3061.
(9) Pant, P. V. K.; Han, J.; Smith, G. D.; Boyd, R. H. *J. Chem. Phys.* **1993**, *99*, 597.
(10) Berendsen, H. J. C.; Spoel, D. v. d.; Drunen, R. v. *Comput. Phys. Comm.* **1995**, *91*, 43.
(11) Lindahl, E.; Hess, B.; Spoel, D. v. d. *J. Mol. Model.* **2001**, *7*, 306.
(12) Berendsen, H. J. C.; Postma, J. P. M.; Gunsteren, W. F. v.; DiNola, A.; Haak, J. R. *J. Chem. Phys.* **1984**, *81*, 3684.
(13) Allen, M. P.; Tildesley, D. J. *Computer Simulation of Liquids*; Clarendon Press: Oxford, England, 1987.
(14) Maya, S. L.; Olafson, B. D.; Goddard, W. A., III. *J. Chem. Phys.* **1990**, *94*, 8897.
(15) Olabisi, O.; Simha, R. *Macromolecules* **1975**, *8*, 206.
(16) Olabisi, O.; Simha, R. *Macromolecules* **1975**, *8*, 211.
(17) Müller-Plathe, F.; Rogers, S. C.; Gunsteren, W. F. v. *Macromolecules* **1992**, *25*, 6722.
(18) Cuthbert, T. R.; Wagner, N. J.; Paulaitis, M. E.; Murgia, G.; D'Aguanno, B. *Macromolecules* **1999**, *32*, 5017.
(19) Harmandaris, V. A.; Mavrantzas, V. G.; Theodorou, D. N. *Macromolecules* **1998**, *31*, 7934.
(20) Müller-Plathe, F. *Macromolecules* **1996**, *29*, 4782.
(21) Fels, M.; Huang, R. Y. M. *J. Appl. Polym. Sci.* **1970**, *14*, 523.
(22) Marklund, E.; Hedenqvist, M. S. Unpublished data.
(23) Vrentas, J. S.; Duda, J. L.; Lau, M. K. *J. Appl. Polym. Sci.* **1982**, *27*, 3987.
(24) Moaddeb, M.; Koros, W. J. *J. Appl. Polym. Sci.* **1995**, *57*, 687.
(25) Matsui, T.; Ono, A.; Shimoda, M.; Osajima, Y. *J. Agric. Food Chem.* **1992**, *40*, 479.

MA0200569